Supporting Information

Efficient and Photostable Ternary Organic Solar Cells with a Narrow Bandgap Non-Fullerene Acceptor and Fullerene Additive

Jinho Lee,[ab ‡] Jong-Hoon Lee,[a ‡] Huifeng Yao,[c] Hyojung Cha,[b] Soonil Hong,[a] Seongyu Lee,[a] Jehan Kim,[d] James R. Durrant,[b] Jianhui Hou[c*] and Kwanghee Lee[a*]

[a] Heeger Center for Advanced Materials and Research Institute for Solar and Sustainable Energies, Gwangju Institute of Science and Technology, Gwangju 61005, Republic of Korea. E-mail: klee@gist.ac.kr

[b] Department of Chemistry and Centre for Plastic Electronics, Imperial College London, London W12 0BZ, UK.

[c] State Key Laboratory of Polymer Physics, Chinese Academy of Sciences, Beijing 100190, China. E-mail: hjhzlz@iccas.ac.cn

[d] Pohang Accelerator Laboratory (PAL), Pohang University of Science and Technology (POSTECH), Pohang 790-784, Republic of Korea

‡ These authors contributed equally to this work.

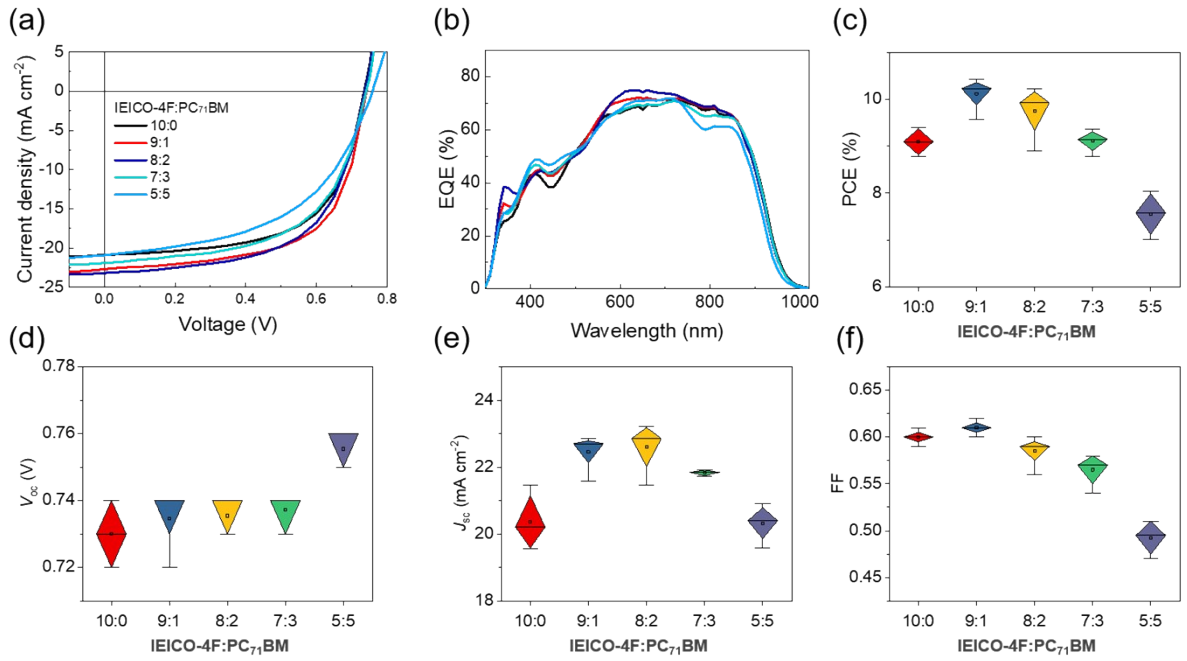

Fig. S1 (a) *J-V* characteristics and (b) EQE spectra of OSCs with different $PC_{71}BM$ contents in the acceptor and corresponding photovoltaic parameters of (c) PCE, (d) V_{oc}, (e) J_{sc}, and (f) FF.

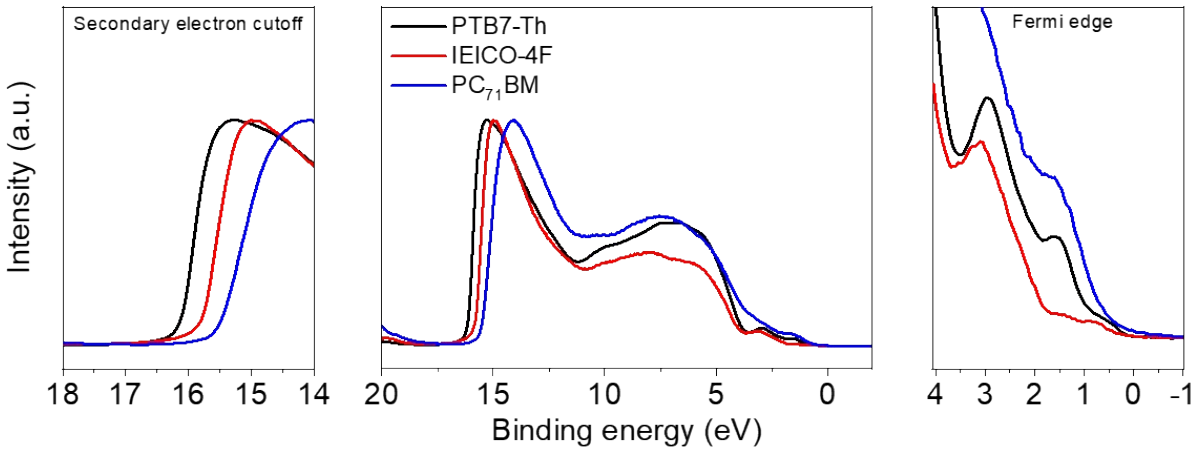

Fig. S2 UPS spectra of PTB7-Th, IEICO-4F, and $PC_{71}BM$ films.

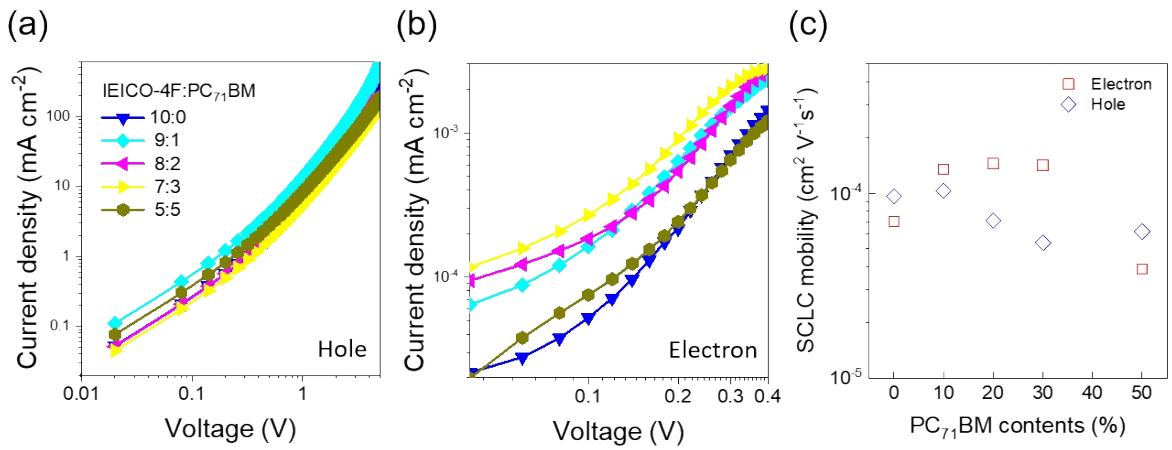

Fig. S3 *J-V* characteristics of the (a) hole and (b) electron-only devices. (c) The SCLC electron and hole mobilities with different weight ratio of $PC_{71}BM$.

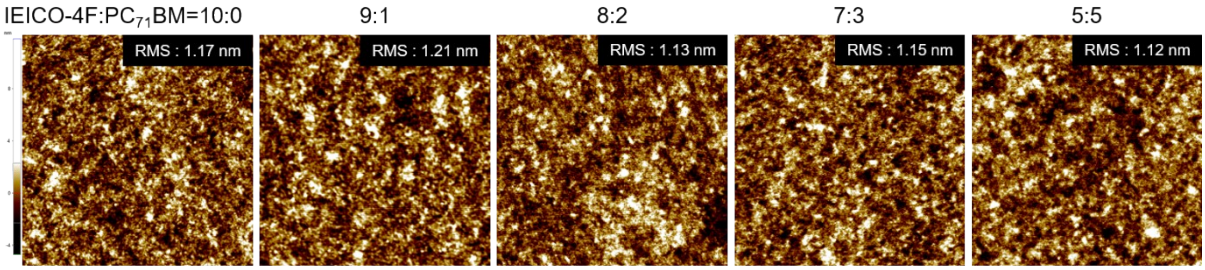

Fig. S4 AFM images for the BHJ blend films with different acceptor ratios deposited on PEDOT:PSS layer.

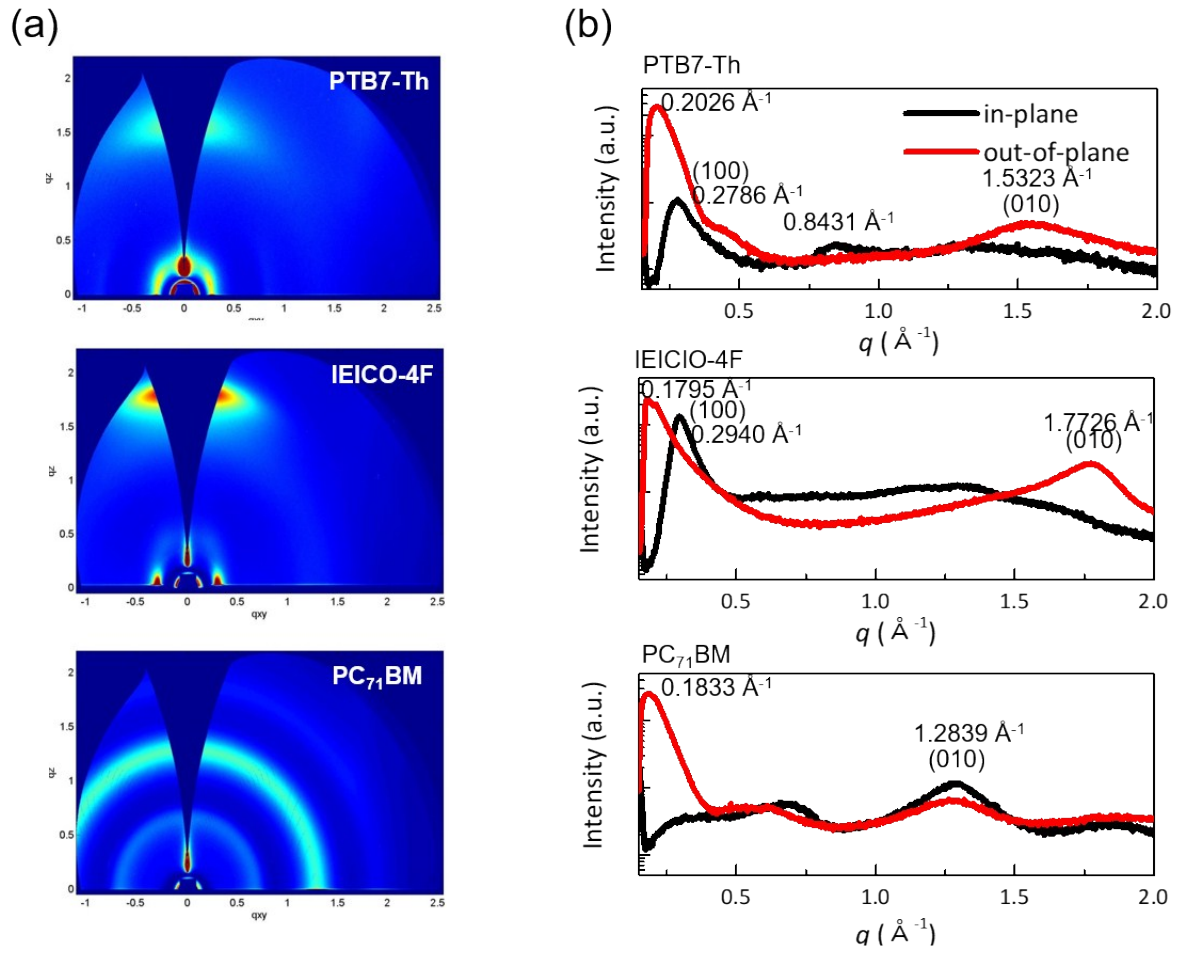

Fig. S5 (a) 2D GIWAXS patterns and (b) corresponding out-of-plane and in-plane scattering profiles of PTB7-Th, IEICO-4F, and $PC_{71}BM$.

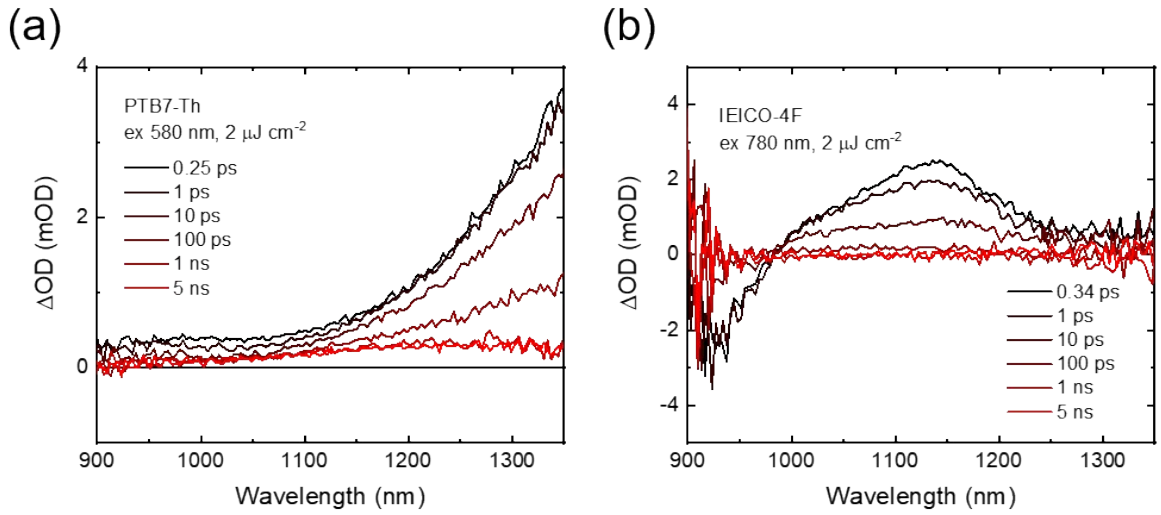

Fig. S6 Transient absorption spectra of (a) neat PTB7-Th and (b) neat IEICO-4F films, following excitation at 580 nm.

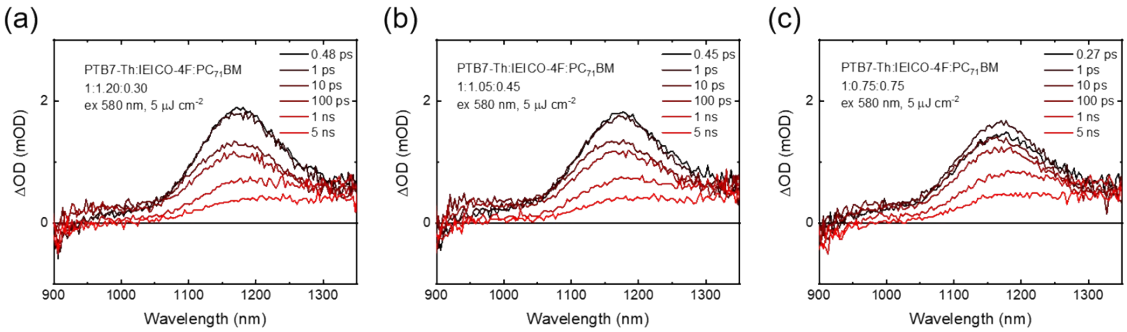

Fig. S7 Transient absorption spectra of PTB7-Th:IEICO-4F:$PC_{71}BM$ ternary blend films with different ratio of (a) 1:1.2:0.3, (b) 1:1.05:0.45, and (c) 1:0.75:0.75, following excitation at 580 nm.

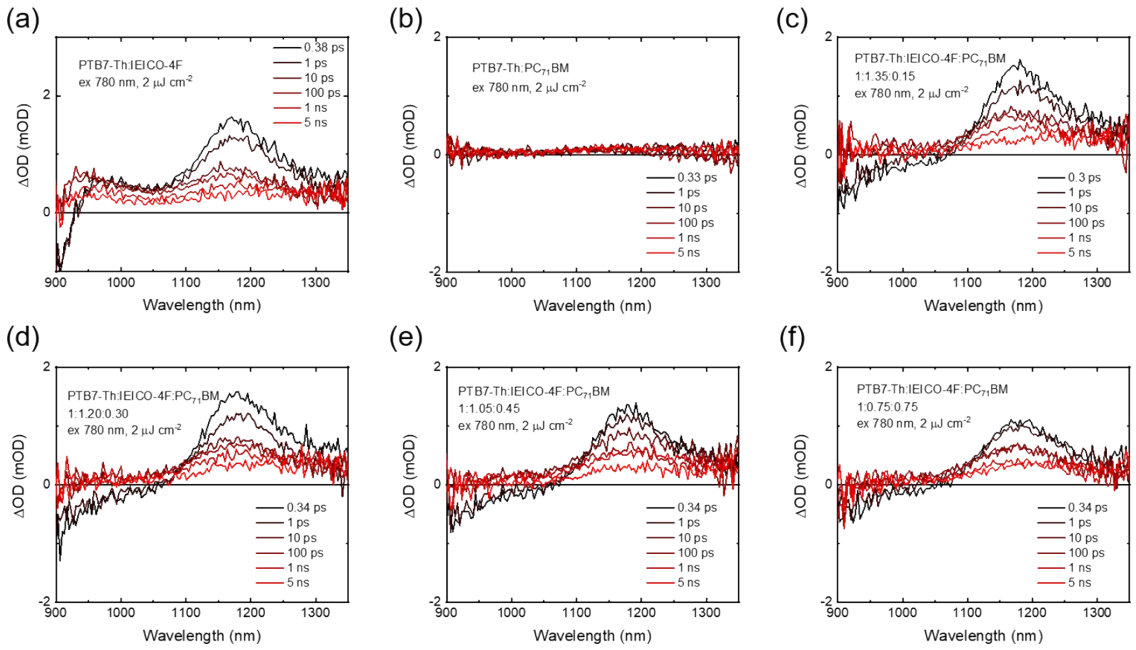

Fig. S8 Transient absorption spectra of (a) PTB7-Th:IEICO-4F and (b) PTB7-Th:$PC_{71}BM$ binary blend films, and PTB7-Th:IEICO-4F:$PC_{71}BM$ ternary blend films with different ratio of (c) 1:1.35:0.15, (d) 1:1.2:0.3, (e) 1:1.05:0.45, and (f) 1:0.75:0.75, following excitation at 780 nm.

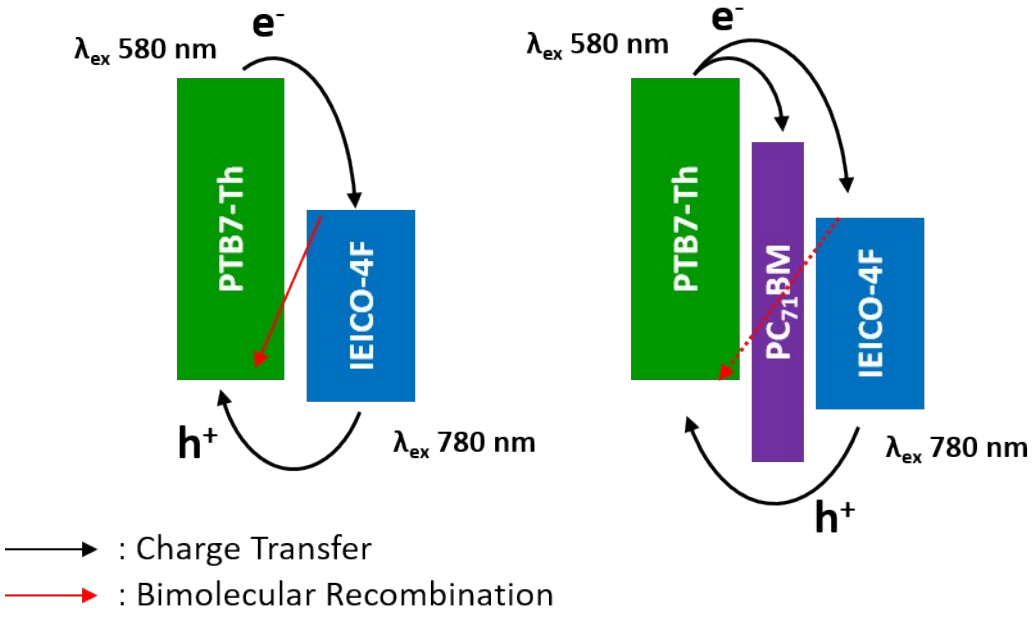

Fig. S9 Schematic energy level diagram of binary and ternary blend systems.

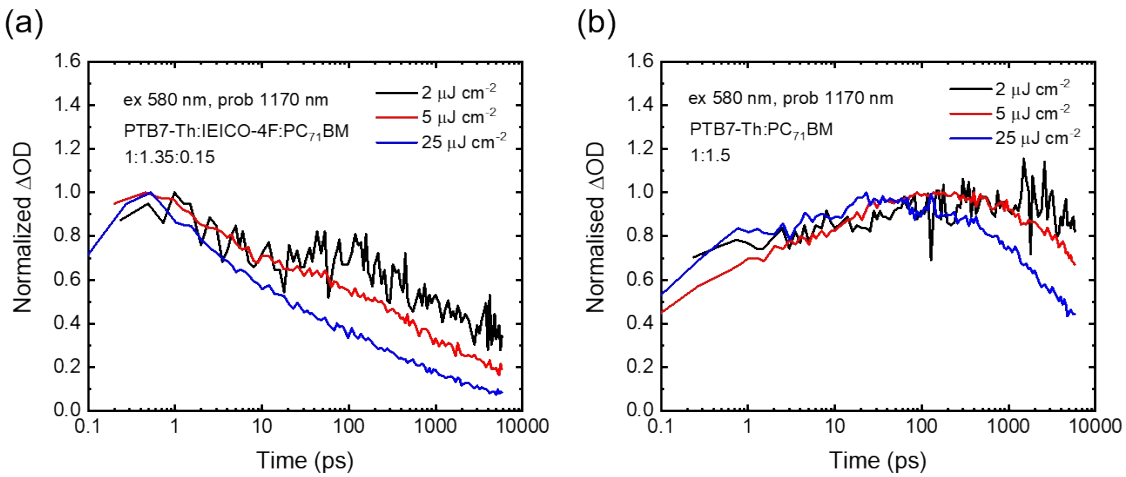

Fig. S10 Decay dynamics probed at 1170 nm as a function of excitation density for (a) PTB7-Th:IEICO-4F:$PC_{71}BM$ (1:1.35:0.15) ternary blend and (b) PTB7:Th:$PC_{71}BM$ (1:1.5) binary blend films.

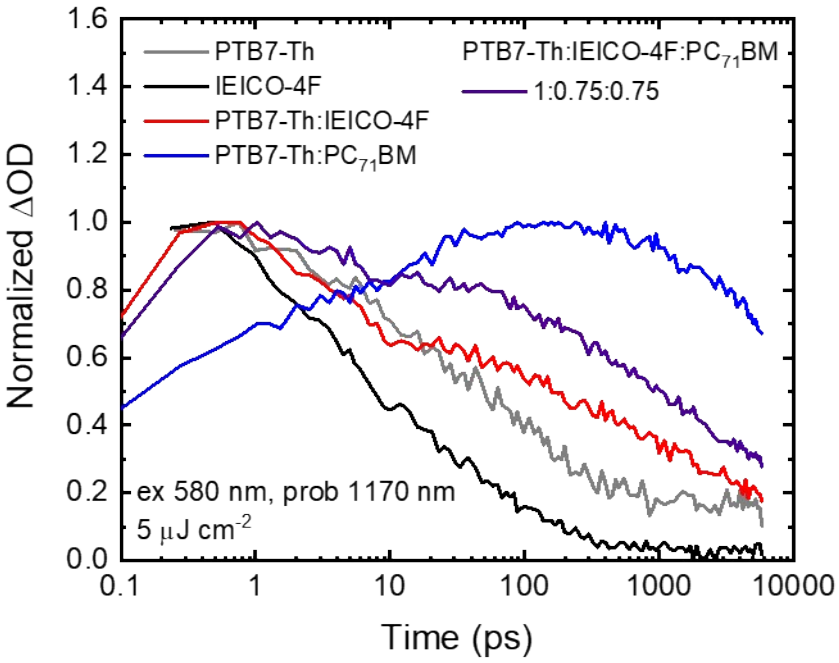

Fig. S11 Blend decay dynamics for various neat and blend films excited at 580 nm and probed at 1170 nm.

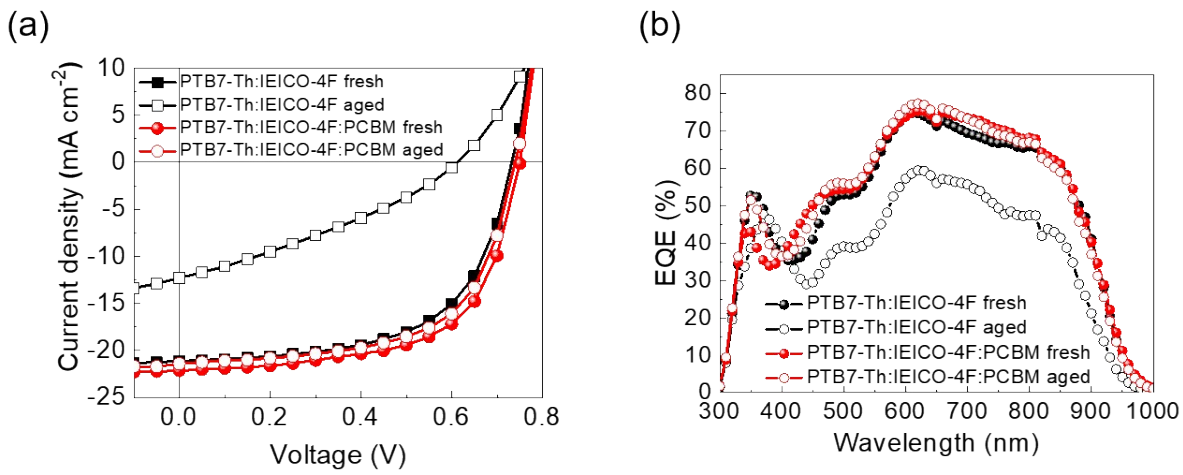

Fig. S12 (a) *J*–*V* characteristics and (b) EQE spectra of fresh and aged devices with binary and ternary blends.

		V_{oc} (V)	J_{sc} (mA/cm^2)	FF	PCE (%)
PTB7-Th: IEICO-4F (1:1.5)	Pristine	0.73	21.15	0.60	9.26
	AM 1.5G light soaking (60 h)	0.61	12.31	0.32	2.41
PTB7-Th: IEICO-4F: $PC_{71}BM$ (1:1.35:0.15)	Pristine	0.75	22.15	0.62	10.31
	AM 1.5G light soaking (300 h)	0.73	21.10	0.60	9.31

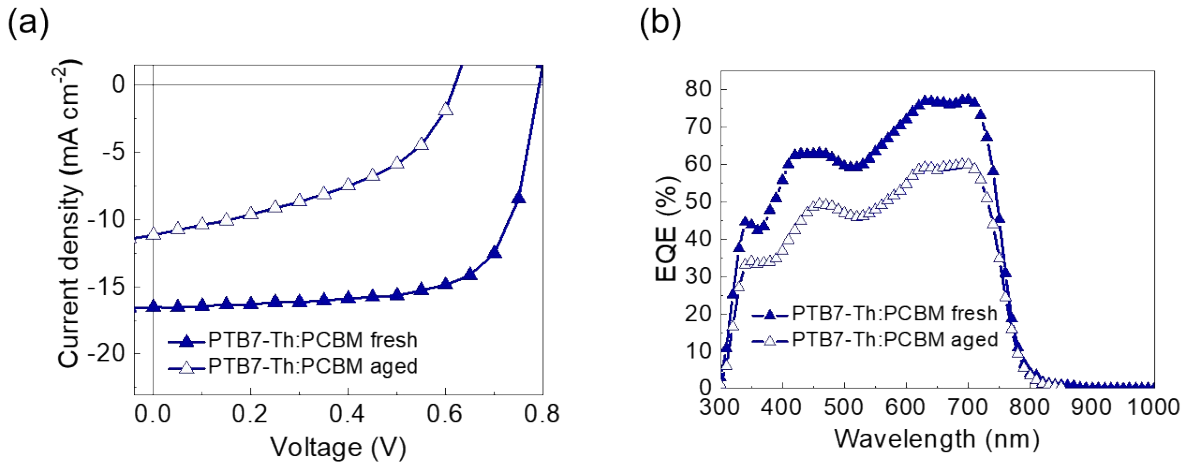

Fig. S13 (a) *J–V* characteristics and (b) EQE spectra of fresh and aged devices with the PTB7-Th:$PC_{71}BM$ photoactive layer.

		V_{oc} (V)	J_{sc} (mA/cm^2)	FF	PCE (%)
PTB7-Th: $PC_{71}BM$ (1:1.5)	Pristine	0.79	16.51	0.70	9.18
	AM 1.5G light soaking (300 h)	0.62	11.14	0.44	3.05

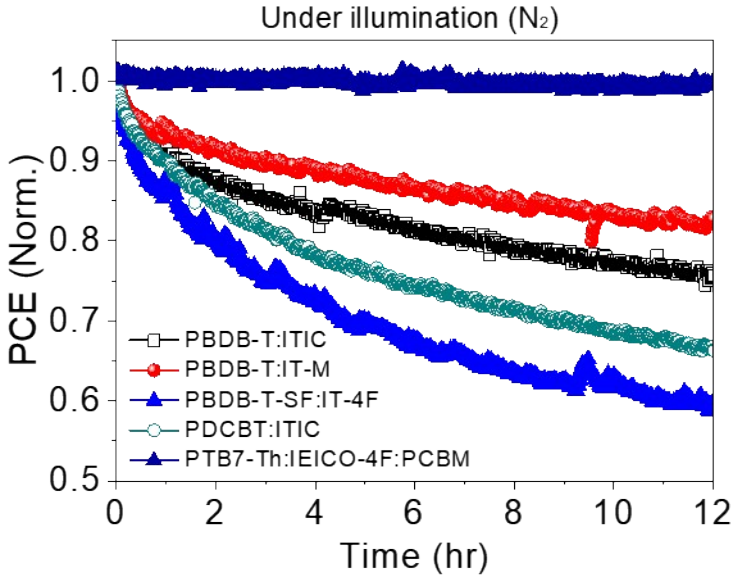

Fig. S14 Photostability of OSCs with various NFA photoactive materials, including PBDB-T:ITIC, PBDB-T:IT-M, PBDB-T-SF:IT-4F, PDCBT:ITIC, and PTB7-Th:IEICO-4F:$PC_{71}BM$ under continuous AM 1.5G illumination (100 mW cm^{-2}) in N_2.

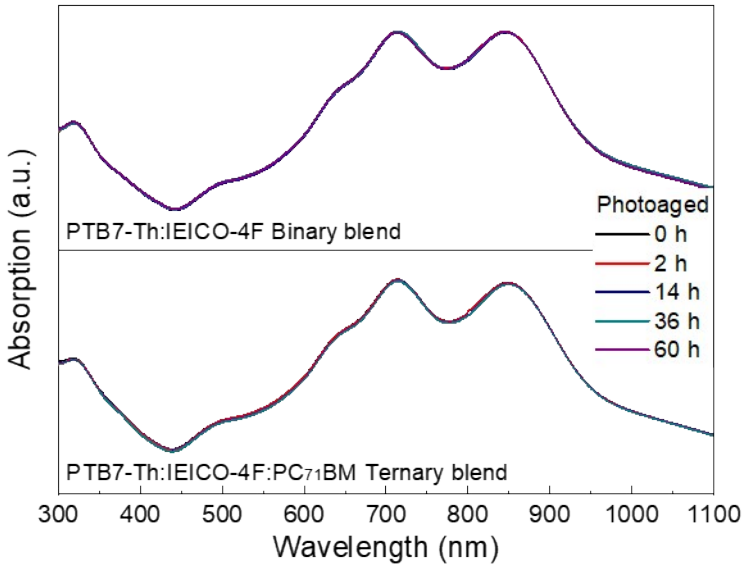

Fig. S15 UV-VIS absorption spectra of binary PTB7-Th:IEICO-4F and ternary PTB7-Th:IEICO-4F:$PC_{71}BM$ films with different light exposure times.

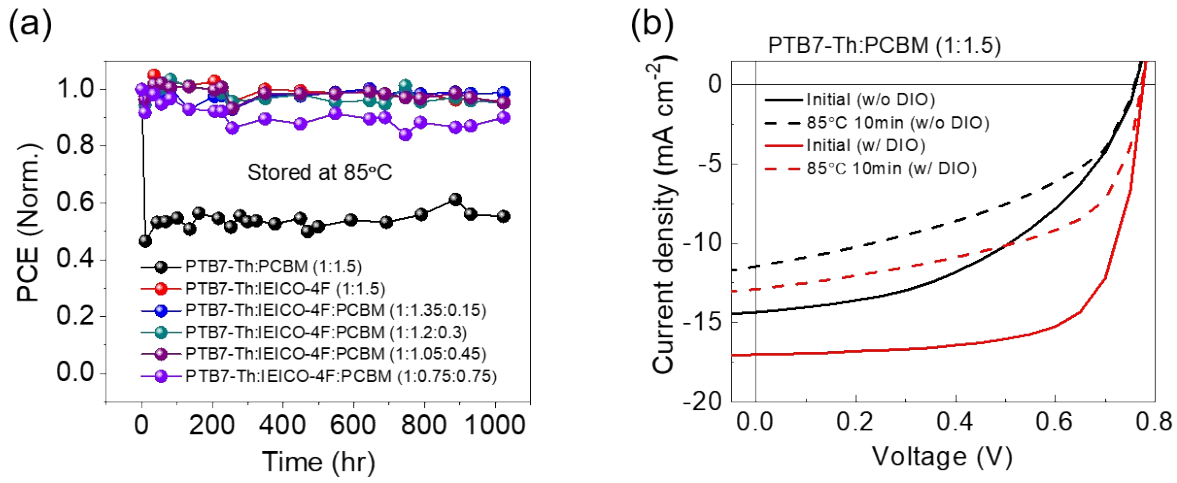

Fig. S16 (a) Thermal stability test of OSCs with various acceptor ratios under continuous 85 °C heat exposure. (b) *J*–*V* characteristics of pristine and thermally annealed PTB7-Th:$PC_{71}BM$ devices.

		V_{oc} (V)	J_{sc} (mA/cm^2)	FF	PCE (%)
PTB7-Th: $PC_{71}BM$ (1:1.5)	Pristine (w/o DIO)	0.76	14.35	0.47	5.08
	85 °C for 10 min	0.76	11.46	0.44	3.79
PTB7-Th: $PC_{71}BM$ (1:1.5)	Pristine (w/ 3% DIO)	0.78	17.03	0.71	9.32
	85 °C for 10 min	0.77	12.91	0.55	5.51

Table S1 The mobility values of electrons, holes and their ratio derived from the SCLC method.

IEICO-4F:$PC_{71}BM$	$\mu_{electron}$ ($\times10^{-4}$ cm^2/Vs)	μ_{hole} ($\times10^{-4}$ cm^2/Vs)	$\mu_{electron}/\mu_{hole}$
10:0	0.713	0.965	0.739
9:1	1.34	1.02	1.32
8:2	1.45	0.712	2.03
7:3	1.42	0.536	2.64
5:5	0.388	0.620	0.63

Table S2 Measured and calculated parameters for understanding charge generation/collection within the devices obtained from the J_{ph}-V_{eff} curves.

	$J_{ph,sc}$* (mA cm^{-2})	$J_{ph,mpp}$* (mA cm^{-2})	J_{sat} (mA cm^{-2})	G_{max} (m^{-3} s^{-1})	$J_{ph,sc}/J_{sat}$ (%)	$J_{ph,mpp}/J_{sat}$ (%)
Binary fresh	20.75	16.13	23.99	1.53×10^{28}	86.5	67.2
Binary aged	11.37	8.14	13.43	8.57×10^{27}	84.7	60.6
Ternary fresh	22.92	18.55	25.29	1.66×10^{28}	90.6	73.4
Ternary aged	21.31	17.18	23.43	1.54×10^{28}	91.0	73.3

*$J_{ph,sc}$ and $J_{ph,mpp}$ represent photocurrent density at short-circuit and maximum power point conditions, respectively.